Buried waveguide in neodymium-doped phosphate glass obtained by femtosecond laser writing using a double line approach

Xuewen Long (龙学文)[1,2], Jing Bai (白 晶)[1,2], Xin Liu (刘 欣)[1,2], Wei Zhao (赵 卫)[1], and Guanghua Cheng (程光华)[1*]

[1] *State Key Laboratory of Transient Optics and Photonics, Xi'an Institute of Optics and Precision Mechanics, Chinese Academy of Sciences, Xi'an 710119, China*

[2] *University of Chinese Academy of Sciences, Beijing 100049, China*

[*] *Corresponding author: gcheng@opt.ac.cn*

Received June 18, 2013; accepted August 2, 2013; posted online September 29, 2013

We fabricate a buried channel waveguide in neodymium-doped phosphate glass using a double line approach by femtosecond laser writing. Raman spectra reveal an expansion of the glass network in the laser irradiated region. Given the stress-induced positive refractive index change, waveguiding between two separated tracks is demonstrated. The refractive index difference profile of the waveguide is reconstructed from the measured near-field mode. Propagation loss is measured by scattering technique. Microluminescence spectra reveal that the Nd^{3+} fluorescence property is not significantly affected by waveguide formation process, which indicates that the inscribed waveguide is a good candidate for active device.

OCIS codes: 230.7380, 140.7090.

doi: 10.3788/COL201311.102301.

Since the pioneering work of Davis *et al.*[1] femtosecond (fs) direct laser writing (FDLW) has attracted considerable interest for integrated, miniaturized three-dimensional (3D) photonics in transparent materials. fs lasers can induce permanent, highly localized regions of refractive index change suitable for the formation of 3D photonic devices including splitters[2], directional couplers[3], gratings[4,5], magneto-optical waveguides[6], and waveguide lasers[7,8] in a range of glasses and crystals. This technique enables the reliable, fast, and low-cost fabrication of 3D photonic devices without the design and fabrication of a complex mask in contrast to most standard fabrication techniques. Accordingly, FDLW has gradually become one of the most popular methods in recent years.

Phosphate glasses are important substrates because they can incorporate high concentrations of rare-earth ions. The ability to possess a high gain per unit length is crucial to miniaturized active devices. Therefore, ultrafast laser 3D photo-inscription in phosphate glasses deserves investigation. Phosphate glasses exhibit positive or negative changes to the index of refraction inside the fs-laser irradiated region depending on initial glass composition[9]. When writing waveguides in transparent materials, two distinct regimes exist. In type I, the modified region exhibits a localized increase in refractive index, and the optical waveguide can be directly generated along the straight line of modification. In type II, the mode is guided in the virtually pristine material neighboring laser damage track. Therefore, type-II waveguides preserve the properties of the original material. Type-II waveguides have been mainly demonstrated in a range of crystals[10–13].

In this letter, we inscribed a buried type-II waveguide in neodymium-doped phosphate glass by writing two parallel lines in close separation. Raman microscopy was used to analyze the laser written track. The Raman peak associated with P-O bonds exhibits a negative shift in wavenumber, which reveals longer P-O bonds and an expansion of the glass network in the fs-laser irradiated region[9]. The stress-induced increase in refractive index between pairs of tracks and depressed refractive index within tracks support efficient light propagation. The waveguide fabricated using a double line approach exhibits propagation loss of 1.2 dB/cm at 980-nm wavelength. The refractive index profile of the buried waveguide is reconstructed. Microluminescence experiments reveal that the original fluorescence of the neodymium-doped glasses is preserved in the guiding regions.

Figure 1 is a schematic of the experimental setup. A transverse writing configuration with the sample translation perpendicular to the laser propagation axis was used throughout the study. To structure the phosphate glass, a commercial amplified Ti:sapphire laser system (Spitfire, Spectra Physics) was used. The system was operated at a repetition rate of 1 kHz and provided pulses at a central wavelength of 800 nm with a minimum pulse duration of 120 fs and pulse energy up to 1 mJ. A

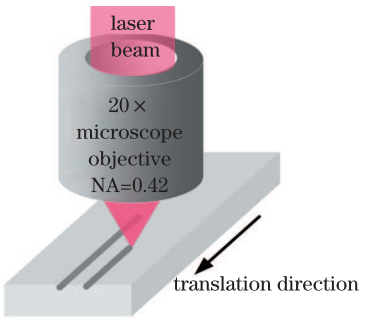

Fig. 1. Schematic representation of the femtosecond laser transversal writing geometry.

continuous variation of the output power was obtained using half a wave plate and a polarizer. Before the objective lens, a computer-controlled shutter is used to control the irradiation time of the laser pulses in the sample. The density and refractive index of the Nd^{3+}-doped phosphate glass (doped with 3 wt-.% Nd_2O_3) are 2.83 g/cm^3 and 1.54, respectively. The size of the sample is 4.0 × 5.0 × 10.0 (mm). All six glass surfaces were optically polished for the convenience of writing and real-time monitoring. A polished phosphate glass cuboid was mounted on a computer-controlled XYZ motion stage (Physik Instrumente) that allowed translation parallel or perpendicular to the laser propagation axis. The laser beam was focused on 300 μm below the surface of the sample using a 20× microscope objective (NA=0.42; Mitutoyo). Two parallel lines were written with a separation of 20 μm by translating the sample with a speed of 50 μm /s and pulse energy of 1 μJ.

After inscribing the waveguide, the end surface of the sample was cut and polished to expose the end facets of the waveguide on the surface. The length of the waveguide was about 9 mm after polishing the end facets of the sample. The optical transmission microscope image of the exit plane of the double line structure is shown in Fig. 2(a). Pulses were focused from the top of the image. The black filaments correspond to the focused laser regions, and the brilliant region between them corresponds to the guiding zone. Figure 2(b) shows a polarizing microscope image of the cross-section of the tracks. Phosphate glass is an optically isotropic material, and thus the polarization of the transmitted light does not change and the picture should be black under crossed polarizers. However, the regions surrounding the tracks appear white, indicating that the polarization of light changes on the way through the sample as a result of stress-induced birefringence. To gain a better understanding of the formation mechanism of the waveguide induced by fs lasers, Raman microscopy was used to analyze the laser written track. The structure of phosphate glasses can be described as a network of phosphate tetrahedra linked through the covalent bonding of corner-shared oxygen atoms referred to as bridging oxygen atoms. Oxygen atoms that do not link two phosphate tetrahedra are called nonbridging. Raman spectroscopy provides information about the molecular-level structure of phosphate glasses. Figure 3 shows the Raman spectra collected from the unexposed bulk phosphate glasses and fs-laser inscribed filament. The large band at 1 209 cm^{-1} originates from the symmetric resonances associated with the O–P–O nonbridging oxygens

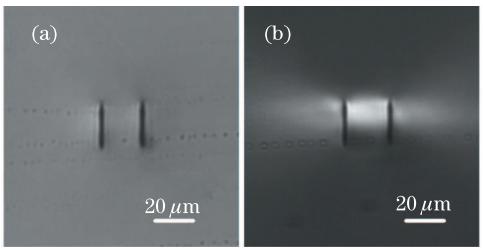

Fig. 2. Optical transmission micrograph of the obtained double line structure (end view). (a) Bright-field image of the cross-section and (b) polarizing microscope image of the cross-section.

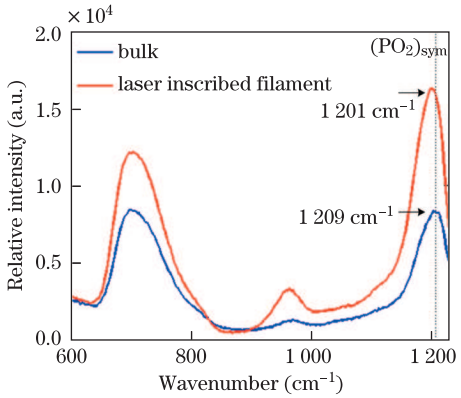

Fig. 3. (Color online) Raman spectra of the unmodified bulk phosphate glass and the inscribed track.

on phosphate tetrahedra, (PO_2)sym[9]. A spectral shift toward lower wavenumber is observed in the laser irradiated filament. The shift can be attributed to an expansion of the glass network ascribed to longer P-O bonds induced by fs-laser irradiation, resulting in lower density and lower refractive index in the fs-laser irradiated filament. Therefore, the unexposed region between double tracks can demonstrate higher refractive index (waveguiding) resulting from compression induced by the expansion of the focus volume. Considering the change in refractive index, waveguiding is possible at the center of the pairs of tracks. Waveguiding experiments were performed by coupling the laser polarized parallel to the long axis of the cross-section of the written tracks at a wavelength of 980 nm into the waveguide with a 20× microscope objective (NA=0.4). The backside of the waveguide was imaged with a 10× microscope objective (NA=0.28) onto a charge-coupled device (CCD) camera. Waveguiding was observed at the center between two adjacent tracks. The guided mode (Fig. 4(a)) in the center of the pair structure has a nearly Gaussian profile. We reconstructed the refractive index profile of the waveguide from near-field mode according to the method described in Ref. [14]. In this method, the distribution of the refractive index change $\Delta n(x, y)$ is given by

$$\Delta n(x,y) = \sqrt{n_s^2 - \frac{1}{k^2 A(x,y)} \nabla_t^2 A(x,y)} - n_s, \quad (1)$$

where ∇_t^2 is the Laplacian operator acting on x and y, $A(x, y)$ is the normalized electric field intensity, k is the wavenumber in a vacuum, and n_s is the refractive index of phosphate glass. A direct relationship exists between the refractive difference index profile of the waveguide and the field distributions of the guided modes according to Eq. (1). Therefore, the refractive index difference profile can be recovered by solving Eq. (1) using the finite difference method. Figure 4(b) shows that the index profile consists of an increased index ($\Delta n_{WG} = +2.2 \times 10^{-4}$) in the waveguide region and a depressed index within the tracks ($\Delta n_F = -1.2 \times 10^{-4}$). The combination of refractive index reduction within the tracks and stress-induced positive refractive index change between the tracks is responsible for excellent confinement of the fundamental mode.

Optical loss is an important parameter for waveguides used in integrated optics. Most transmission losses of

double line waveguides are due to scattering arising from the roughness of filaments. Waveguide propagation loss was measured by the scattering technique at a wavelength of 980 nm[15,16]. The exponential fall-off of the scattered light out of the optical waveguide was recorded with a CCD camera transversely positioned to the sample. This decay follows an exponential form according to $I_L = I_0 \exp(-\alpha L)$, where I_L is the scattered intensity after a propagation length L through the waveguide, I_0 is the initial intensity at the start of the path, and α is the loss coefficient to be determined. The above equation can be rewritten in the form $\ln(I_L) = \ln(I_0) - \alpha L$. Therefore, by recording the scattered intensity along the waveguide and using the linear fit to the data based on the above equation, we can readily determine the loss coefficient. To avoid the influence of strong scattering at the input and output facets on measurement accuracy, the 3-mm-long streak scattered out of the middle area of the waveguide was selected for loss evaluation. Figure 5 shows the data extracted from the scattered light image recorded from the waveguide and the fit profile. The slope of linear fit profile represents the loss coefficient. In this case, the propagation loss of the waveguide is 1.22 dB/cm (i.e., $\alpha = 0.28$ cm^{-1}). This value is the same order of magnitude of the propagation losses for fs-laser-written double line waveguides in most crystals and acceptable for applications in integrated optical circuits requiring wave transmission over relatively short lengths (e.g., several millimeters).

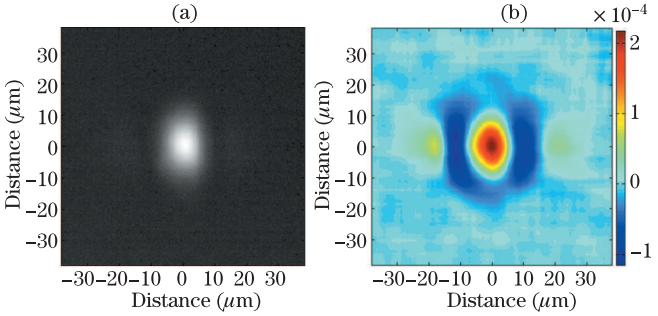

Fig. 4. (a) Near-field mode of the waveguide; (b) calculated relative refractive index distribution of the waveguide corresponding to the near-field mode presented in (a).

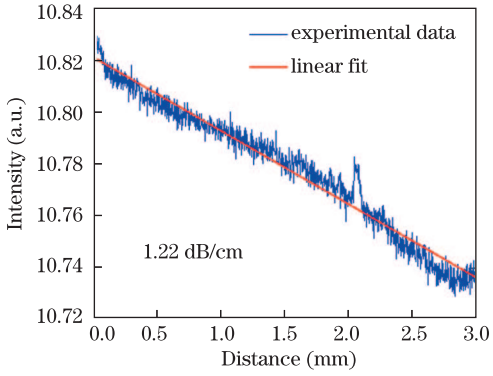

Fig. 5. (Color online) Propagation loss evaluation based on the decay of scattered light.

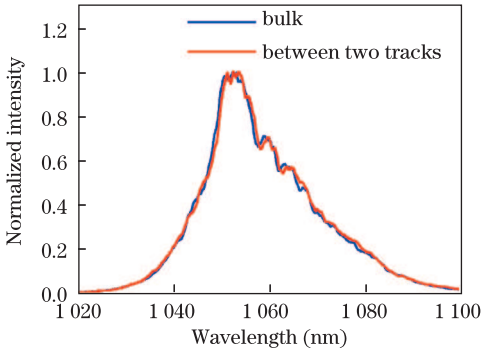

Fig. 6. (Color online) Fluorescence spectra of the bulk material (blue) and the central region between two tracks (red).

To analyze the suitability of the obtained optical waveguide as an integrated active device, how the spectroscopic properties of the active Nd^{3+} ions are affected by the waveguide fabrication procedure must be deterimed. For this purpose, microluminescence experiments were carried out. The light of a Ti:Sapphire laser system operating at a wavelength of 808 nm was focused with a 40× microscope objective on the surface of the neodymium-doped phosphate glass to excite the neodymium ions to the $^4F_{5/2}$ level. The $^4F_{3/2} \rightarrow {}^4F_{11/2}$ fluorescence was collected by the same objective and deflected using a dichroitic mirror into a spectrometer with a resolution of 0.1 nm. The mirror is highly reflective within the wavelength range of 1 020–1 100 nm and antireflective at the wavelength of 808 nm. Figure 6 shows the resulting normalized emission spectra. The blue line indicates the spectrum of the unmodified bulk region of phosphate glass. To examine the guiding zone between two 20-μm separated tracks, the central region of the two-track structure was excited. The resulting spectrum is drawn in red in Fig. 6. Both spectra are very similar, including the shape and peak position, revealing that the fluorescence properties of Nd^{3+} ions are not significantly affected by the waveguide formation process. Thus, the fabricated structures are promising candidates for the future development of integrated active devices.

In conclusion, we demonstrate a buried channel waveguide in neodymium-doped phosphate glass produced by a low-repetition-rate fs laser. Raman spectra show an expansion of the glass network in the laser irradiated tracks. The combination of refractive index reduction within the tracks and stress induces a positive refractive index change between double-track support guiding. A propagation loss of 1.2 dB/cm is determined by registering the scattering light from the top of the guiding structures. The refractive index profile of the waveguide is reconstructed based on the near-field mode. Microluminescence spectra of the waveguide show that the fluorescence properties of Nd^{3+}ions are not significantly affected by waveguide formation, which indicates a fairly good potential for further laser actions in a compact device.

The work was supported by the West Light Foundation of the Chinese Academy of Sciences and National Natural Science Foundation of China (No. 61223007).

References

1. K. M. Davis, K. Miura, N. Sugimoto, and K. Hirao, Opt. Lett. **21,** 1729 (1996).
2. D. Homoelle, S. Wielandy, and A. Gaeta, Opt. Lett. **24,** 1311 (1999).
3. A. M. Streltsov and N. F. Borrelli, Opt. Lett. **26,** 42 (2001).
4. C. Voigtländer, D. Richter , J. Thomas, A.Tünnermann, and S. Nolte, Appl. Phys. A **102,** 35 (2011).
5. Y. Wang, Y. H. Li, and P. X. Lu, Chin. Phys. Lett. **27,** 044213 (2010).
6. Y. Li, X. Gao, M. Jiang, Q. Sun, and J. Tian, Chin. Opt. Lett. **10,** 102201 (2012).
7. A. G. Okhrimchuk, A. V. Shestakov, I. Khrushchev, and J. Mitchell, Opt. Lett. **30,** 2248 (2005).
8. C. Zhang, N. Dong, J. Yang, F. Chen, J. R. Vázquez de Aldana, and Q. Lu, Opt. Express **19,** 12503 (2011).
9. L. B. Fletcher, J. J. Witcher, N. Troy, S.T. Reis, R. K. Brow, and D. M. Krol, Opt. Express **19,** 7929 (2011).
10. X. Liu, S. Qu, Y. Tan, C. Zhang, and F. Chen, Appl. Phys. B **103,** 145 (2011).
11. W. F. Silva, C. Jacinto, A. Benayas, J. R. Vazquez de Aldana, G. A. Torchia, F. Chen, Y. Tan, and D. Jaque, Opt. Lett. **35,** 916 (2010).
12. S. J. Beecher, R. R. Thomson, D. T. Reid, N. D. Psaila, M. Ebrahim-Zadeh, and A. K. Kar, Opt. Lett. **36,** 4548 (2011).
13. F. Chen and J. R. V'azquez de Aldana, Laser Photon. Rev. **1,** 26 (2013).
14. F. Caccavale, F. Segato, I. Mansour, and M. Gianesin, J. Lightwave Technol. **16**, 1348 (1998).
15. Y. Okamura, S. Yoshinaka, and S. Yamamoto, Appl. Opt. **22,** 3892 (1983).
16. H. Zhang, S. M. Eaton, and P. R. Herman, Opt. Express **14,** 4826 (2006).